*Biochimica et Biophysica Acta*, 1064 (1991) 212–218

*ADONIS* 000527369100189U

BBAMEM 75207

# Subconductance states in calcium-activated potassium channels from canine airway smooth muscle

Lisa L. Stockbridge [1], Andrew S. French [1] and S.F. Paul Man [2]

[1] *Department of Physiology, University of Alberta, Edmonton (Canada) and* [2] *Department of Medicine, University of Alberta, Edmonton (Canada)*

(Received 15 October 1990)

Key words: Potassium ion channel; Smooth muscle; Subconductance

**The single-channel patch clamp technique was used to analyze subconductance states in the 260 pS calcium-activated potassium channel from canine airway smooth muscle. More than sixty minutes of single channel data (> 87000 events) from five excised patches were analyzed. Six subconductance amplitudes were clearly established to be 17, 33, 41, 52, 63 and 72% of the full conductance. Subconductance openings were usually brief (milliseconds) and represented less than 5% of the total channel open time, but they also persisted for several seconds on rare occasions. They appeared to be unaffected by voltage or time after seal formation, but may have increased in occurrence with decreasing calcium concentration. Irregular amplitude intervals, and the presence of ramp-like, analog transitions between conductance states, suggest a model for maxi-K subconductance states in which the channel protein undergoes random conformational changes causing a variable pore size.**

## Introduction

Subconductance states, apparent openings to less than the full open conductance state, have now been described in many ion channels including large calcium-activated potassium (maxi-K) channels [1–8]. Unlike chloride channel subconductance states which seem to occur frequently [9–12], subconductance state occurrence in maxi-K channels is usually infrequent. Therefore, subconductance states have been generally disregarded in constructing kinetic models for the maxi-K channel [2,4,5,7,13,14]. As longer channel records are examined for better kinetics measurements, it has become increasingly clear that maxi-K channels spend a small, but significant, fraction of total open time in subconductance states and this must be considered in models of channel behavior. Unfortunately, the time required to characterize subconductance states by visual inspection is very large and there are no satisfactory methods to automate the process because the phenomenon is not sufficiently understood. It is also difficult to incorporate subconductance states into standard kinetic models when they are found to exist. This paper, although qualitative in nature, attempts to classify subconductance states for the maxi-K channel found in airway smooth muscle [15].

Correspondence: L.L. Stockbridge, Department of Physiology, 7-55 Medical Sciences Building, University of Alberta, Edmonton, Alberta, T6G 2H7 Canada.

## Materials and Methods

Smooth muscle cells from canine trachealis muscle were used. Trachealis muscle was obtained within minutes after the animal was killed. The isolation procedure used was modified from that described by McCann and Welsh [15] and Marthan et al. [16]. Trachealis muscle (approx. 20 mg wet weight), with most of the connective tissue dissected away, was first cut into small bundles and then finely minced. The minced tissue was washed several times with Hank's solution using gentle mechanical agitation. The tissue was then transferred to 10 ml of freshly prepared enzyme solution consisting of collagenase (37 units/ml, highly purified Type IV, Sigma) and elastase (2 units/ml, highly purified Type IV, Sigma) in Hank's solution with a calcium concentration of 0.1 mM. This solution was supplemented with bovine serum albumin (10 mg/ml), penicillin (100 units/ml) and streptomycin (100 μg/ml). The tissue was allowed to incubate at 37°C with mechanical agitation for 2 h. The cell suspension was filtered through a double layer of sterile surgical gauze and centrifuged for

15 min at 200 × g. This was followed by two additional washes with M199 supplemented with 10% fetal bovine serum. The cell suspension was then removed and the cells were plated at approx. $2.5 \cdot 10^4$ cells/cm$^2$ in 35 mm Falcon culture dishes coated with poly(L-lysine). The plates were incubated at 37°C and 6% $CO_2$ in air. After about 1 h, most of the cells had adhered to the plate and were ready for patch clamp study.

Using Trypan blue exclusion, the viability of the cells was > 90%. The cells showed contraction upon exposure to acetylcholine ($10^{-4}$ M). These spindle-shaped cells were easily identifiable.

Cells were used less than 24 h after dissociation and plating to assure minimal de-differentiation [17]. Data were obtained from excised inside-out ($n = 4$) and outside-out ($n = 1$) patches using standard patch clamp techniques [18]. Thick-walled borosilicate microfilament glass was used to fabricate pipettes with resistance values of 16–20 megohms. Pipette tips were coated with Sylgard (Dow Corning) and polished in a microforge. Seal resistances were greater than 10 gigaohms.

The pipette solution for all experiments was (mM): 140 $K^+$, 0 $Ca^{2+}$, 0.5 $Mg^{2+}$, 10 Hepes (pH 7.2), 10 glucose. Calcium was excluded to facilitate the formation of gigaohm seals. Symmetrical potassium solutions (K = K) used in the bath contained (mM): 140 $K^+$, 1.2 $Mg^{2+}$, 10 Hepes (pH 7.2), 10 glucose, and calcium buffered to the desired concentration ($10^{-3}$ to $10^{-8}$ M range) with EGTA [19]. Hepes-buffered saline (HBS) contained (mM): 135 $Na^+$, 5 $K^+$, 1.2 $Mg^{2+}$, $10^{-3}$ $Ca^{2+}$, 10 Hepes (pH 7.2), and 10 glucose. All experiments were performed at room temperature (20–22°C).

Single-channel events were recorded with a List EPC-7 patch clamp amplifier and all potentials are reported with respect to the cell exterior being zero. The output was filtered at 10 kHz bandwidth with a 3-pole Bessel filter and fed into a Medical Systems PCM-1 digital VCR recorder adaptor which digitized and stored events on a Sony Betamax VCR. A digital computer sampled the data at 20 kHz with a 12-bit analog-to-digital convertor. Sampled data was further filtered to 2–5 kHz with a Gaussian digital filter. Records for subconductance state analysis were filtered at 5 kHz. We found no significant changes in subconductance state appearance when filtering at 2 kHz. However, stronger filtering (i.e. to 1 kHz) severely altered the ability to detect the subconductance states and changed their apparent amplitudes.

Single-channel current amplitudes for fully open and subconductance states were measured by direct inspection of the digitized data on a Compaq 386 graphics terminal with the aid of horizontal cursor bars. Goldman-Hodgkin-Katz (GHK) current equations [20], fitted to current amplitude data with a minimum square error technique, were used to determine channel conductance and ion selectivity. These reduce to a linear conductance relationship in symmetric 140 mM potassium solutions and could be fitted by linear regression analysis.

For the determination of open probability ($P_N$), an automated method was used. After an estimate of full conductance was determined, the half-amplitude of this value was used as a threshold to discriminate open and closed states throughout the record. A moving average algorithm corrected for any baseline drift. The mean channel amplitude was then obtained from the mean of the distribution of amplitudes during all openings longer than the filter deadtime. $P_N$ was determined by dividing the total time a channel was in the open state by the total sample time. (In the case of a single channel patch, $P_N$ reduces to the open probability for the channel, $P_{open}$.) Since this method will only measure openings over 50% of full conductance, openings to subconductance states less than 50% of full conductance were added to the total open time of the channel before determining $P_N$. These openings were measured directly from the graphics terminal.

The number of maxi-K channels in a patch was determined under conditions where $P_N$ for the patch was saturated. This involved holding the patch at a positive voltage (e.g. +60 mV) in a bath containing a high calcium concentration (i.e. $10^{-3}$ to $10^{-6}$ M). The maximum number of full conductance openings was then taken as the total number of channels in the patch.

Experiments averaged 1 h in length. For the five experiments reported here, approximately 60 min of channel openings and closings under various conditions were analyzed in detail. Within this time there were over 87000 events larger than 50% of the full conductance, which, taken with subconductance amplitudes smaller than this, accounted for 15 min of the data.

## Results

The conductance and calcium sensitivity of the maxi-K channel from airway smooth muscle (not shown) were similar to the results previously reported by McCann and Welsh [15]. The channel had a mean conductance of 268 ± 15 pS in HBS and 238 ± 6 pS in symmetric potassium solutions. Strong rectification in HBS reflected the high selectivity of this channel for potassium over sodium. The channel exhibited a sigmoidal voltage sensitivity. There was great variability in calcium sensitivity, but $P_{open} = 0.5$ occurred at 0 mV between $10^{-7}$ and $10^{-8}$ M calcium, placing this channel in a subpopulation of maxi-K channels which are very sensitive to calcium (see, for example, Ref. 21).

Six subconductance levels consistently appeared with mean open amplitudes of 17, 33, 41, 52, 63 and 72% of the full open level. The standard deviation for any of these levels measured at all calcium concentrations ($10^{-3}$ to $10^{-9}$ M) and voltages (−150 to +140 mV) did not

exceed 2%. Subconductance states were always seen accompanying full conductances. Subconductance states appeared to have the same selectivity for potassium and sodium since they exhibited the same reversal potential as the full conductance and rectified in a similar manner in HBS. Fig. 1 shows a set of sample traces containing subconductance states. Any of the subconductance states could appear under any of the experimental conditions in which there were channel openings and each channel could exhibit all of the subconductance states. The collection in Fig. 1 was assembled from data taken at different holding voltages and bath solutions. Subconductance states are shown in both long (left side) and short (right side) time frames. They were sometimes associated with fast flickering (e.g. 63%, left side) and sometimes associated with relatively slow transitions (e.g. 33%, left side). Subconductance states were not associated with buzz modes [14]. During such high frequency events, we observed the channel opening to full conductance.

A histogram of occurrence for each subconductance level is shown in Fig. 2. Total % occurrence is derived from the time spent in each subconductance level divided by the total open time for each of the five experiments in all calcium concentrations and voltage conditions. This helped to normalize for the numbers of channels in the patches. The numbers of channels in each patch (left to right) were 1, 7, 5 (outside-out patch), 3 and 5, respectively. The occurrence of the 17% subconductance state may be underestimated due to the difficulty of detecting such small amplitude events. Excluding this, no subconductance state appeared significantly more than any other. This was determined with paired $t$-tests where $P > 0.1$ for all conditions except pairs with the 72% subconductance state. For this subconductance state, $P$ was always larger than 0.07. Occasionally, the channel would spend several seconds opening mainly to one subconductance level. This incident accounts for the off-scale bar at 72% in Fig. 2 and contributed to the lower $P$ value obtained in the paired $t$-tests.

The effect of voltage and calcium on subconductance state occurrence is shown in Fig. 4. To normalize this data for the voltage and calcium dependence of the channel and the numbers of channels in the patches, the time that the channel was open to a subconductance state was divided by the total channel open time to give the % of time in all six subconductance states for each data point. The voltage range for these experiments was $-120$ to $+80$ mV. The calcium concentrations examined were $10^{-3}$, $10^{-6}$, $10^{-6.5}$, $10^{-7}$, $10^{-7.5}$ and $10^{-8}$ M. The data points are depicted in bold. The mean ($\pm$S.E.) sample period was $14292 \pm 1872$ ms ($n = 56$ points). The order of exchanges (low to high calcium and vice versa) varied and did not affect $P_N$ unless the concentration was below $3.5 \cdot 10^{-8}$ M. Sometimes, un-

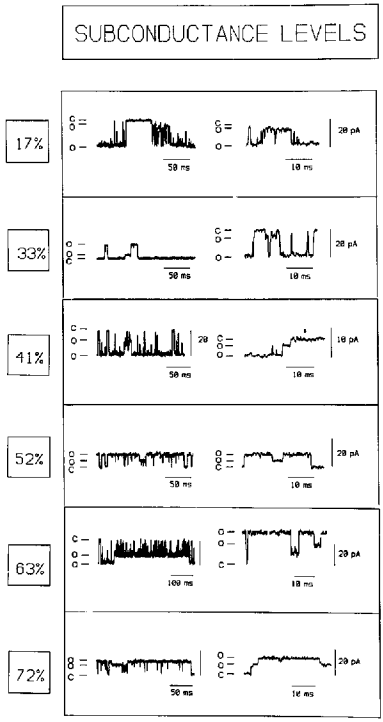


Fig. 1. Samples of 17, 33, 41, 52, 63 and 72% subconductance states recorded at long (left side) and short (right side) time scales. Holding voltages (from top to bottom left side) were $-60$, $+50$, $-60$, $+50$, $-60$ and $+60$ mV, respectively, and (from top to bottom right side) $-40$, $-60$, 0, $+50$, $+70$ and $+60$ mV, respectively. Bath solutions (from top to bottom left side) were $10^{-7}$ M $Ca^{2+}$ K = K, $10^{-8}$ M $Ca^{2+}$ K = K, $10^{-6}$ M $Ca^{2+}$ K = K, $10^{-7}$ M $Ca^{2+}$ K = K, 1.8 mM $Ca^{2+}$ HBS and $10^{-6}$ M $Ca^{2+}$ K = K, respectively, and (from top to bottom right side) $10^{-7}$ M $Ca^{2+}$ K = K, $10^{-6}$ M $Ca^{2+}$ K = K, 1.8 mM $Ca^{2+}$ HBS, $10^{-7}$ M $Ca^{2+}$ K = K, $10^{-6}$ M $Ca^{2+}$ HBS (outside-out patch) and $10^{-8}$ M $Ca^{2+}$ K = K, respectively. Outward current is upwards for all recordings (c = closed, o = opening). Some of the samples contain other subconductance states as well as the one being demonstrated. This is most evident in the sample for the 63% subconductance state (right side) which also shows a 33% subconductance level. All data were filtered at 5 kHz.

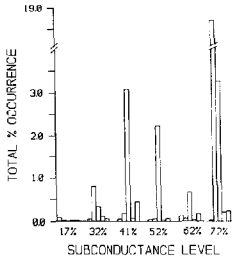


Fig. 2. Histogram of the occurrence for each subconductance level. Total % occurrence is derived from the time spent in each subconductance level divided by the total open time for all calcium concentration and voltage conditions. The individual patches (bars from left to right) contained 1, 7, 5 (outside-out patch), 3 and 5 channels, respectively.

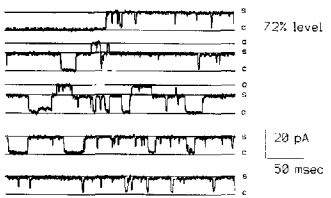


Fig. 3. Single-channel record from an inside-out patch taken during an unusually long period in which the channel spent most of its time opening to the 72% subconductance level. The channel was held at +60 mV in $10^{-8}$ M $Ca^{2+}$ K = K. The current was outward under these conditions (c = closed, s = opening to 72% subconductance state, o (top) = full conductance openings). A 1 kHz filter was used to produce this figure.

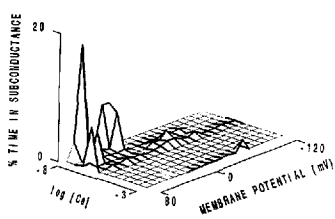


Fig. 4. The effects of holding voltage and calcium concentration on the amount of time spent in subconductance states. Each bold point ($n = 56$) depicts the total time spent in subconductance states divided by the total open time for all experiments at that particular calcium concentration and holding voltage. The mean (±S.E.) open time examined for each point was 14292±1872 ms. There was no significant effect of voltage on subconductance occurrence, although there may be an effect of calcium (see text).

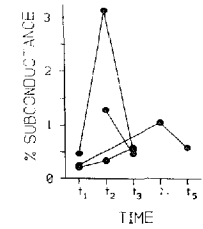


Fig. 5. The effect of time on subconductance state appearance for four inside-out patches. Time bins ($t_1$, $t_2$, etc.) are approximately 12 min each and include data from several voltages and/or calcium concentrations. Although there was a trend for subconductance state occurrence to increase slightly between $t_1$ and $t_2$, there was no progressive effect over the duration of the experiments.

der these conditions, there was a significant increase in subconductance state occurrence followed by a gradual loss of full conductance events that was not completely reversible. Therefore, we must be cautious in interpreting the data from the lowest two calcium concentrations in the figure. There seems to be no effect of voltage on subconductance state occurrence, but there may be some effect of calcium concentration. More data within the $10^{-6.5}$ to $10^{-7.5}$ M range would be required to establish significant effects.

The duration of the experiment was also considered to be a candidate for increasing subconductance state occurrence. In Fig. 5 each time bin ($t_1$–$t_5$) represents a 10–15 min time interval in which a current-voltage relationship was determined and/or a solution exchange was carried out. % subconductance was the total time in all subconductance states divided by the total open time for each bin. Although there was a slight increase in subconductance state occurrence within 20 min after patch excision, this did not seem to progress further during the remaining 60–90 min of each experiment. This indicates that subconductance state occurrence was not an artefact of slow damage to the membrane or channel degradation taking place during the period of experimentation. This finding was further supported by our failure to see any indication of channel rundown in these experiments.

Subconductance states occurred within a range of time scales (see Fig. 1). They were usually seen as square events of diminished amplitude, leading toward a full conductance opening or a full closing. However, on several occasions the current appeared to change smoothly and approximately linearly from one subconductance state to another conductance (full, subconductance or closed). Examples of such analog changes are shown in Fig. 6. Each conductance state had analog events leading to it and/or from it. These instances

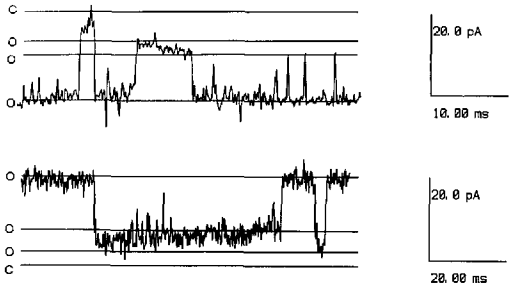


Fig. 6. Samples of analog changes between subconductance states. (Top) A channel in an inside-out patch held at −60 mV in $10^{-7}$ M $Ca^{2+}$ K = K saline. There is an analog shift from 33% to 41% subconductance state. A 2 kHz filter was used for this trace. (Bottom) A channel in an outside-out patch held at +60 mV in $10^{-6}$ M $Ca^{2+}$ HBS saline. There is an analog shift from the 17% to the 41% subconductance state. A 5 kHz filter was used for this trace. Horizontal guides indicate the closed level (c) and sub- and full conductance levels (o).

were always flanked by square events which reduced the possibility that they were artefactual.

## Discussion

Several criteria which have previously been used to define subconductance states [9,22] are met by our data: (1) Subconductance states only appeared under conditions in which there were also full conductance openings. (2) Subconductance states were most often seen leaving a fully closed or fully open state. (3) Subconductance states had the same voltage and calcium sensitivity as the full conductance. (4) Subconductance states appeared to have the same ion selectivity as the full conductance. (5) Under conditions where only one channel was open in the patch, events greater than full conductance were never seen. Although this definition may be too limited for some situations [9], concurrence with these points argues strongly against the possibility that our subconductance states were actually separate channels in the same patch.

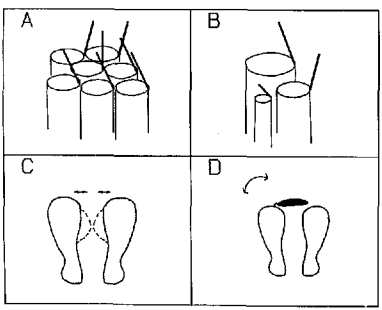


Fig. 7. Possible models for a channel exhibiting subconductance states. Oligopore types may have similar (A) or dissimilar (B) pore diameters. Monopore types may have variable pore size (C) caused by diameter changes or binding properties, or variable gating frequencies (D).

Subconductance state occurrences in airway smooth muscle maxi-K channels appeared to be due to infrequent random events. We found no association between subconductance state occurrence and voltage, but a calcium effect could not be ruled out. For some other channels, subconductance state occurrence has been reported to increase with the duration of the experiment [10] or decrease substantially after seal formation [8]. These types of changes might suggest some sort of artefactual increase in subconductance state occurrence associated with patch excision. However, we found no significant changes in subconductance state occurrence after seal formation.

*Models of subconductance states*

Four models which could explain the occurrences of subconductance states are shown in Fig. 7 and considered here:

(A) In an oligopore channel model, the maxi-K channel would be an aggregate of seven pores of equal size which have a strong cooperativity, but which occasionally function separately. Oligopore models similar to this have been used to describe chloride channels [10,11], sodium channels [23] and potassium channels [24,25] with equidistant subconductance states. Although the oligopore model has also been used to describe maxi-K subconductance states [8], our results

are not compatible with this model because of the irregular subconductance intervals. The first sub-level that we distinguished occurred at approximately 17% followed by intervals of 16%, 8%, 11%, 11%, and 9%, respectively, all with $\leq 2\%$ standard deviation.

(B) A variation of the oligopore model would contain pores of unequal size. With three pores, such a model would give six subconductance levels with irregular intervals. However, there is no set of three unit pore sizes which would explain our subconductance levels. A similar model with more pores could be constructed to explain the intervals which we observed. Such a model would have to exhibit significant flux interaction among neighboring pores to yield the observed number of subconductance levels, yet it is plausible [23]. Analog events would not be explained by this model.

(C) The channel could have a single pore, with conformational changes in the protein giving it a variable pore size. Conformational changes might occur randomly or may be induced by the binding of a ligand to an allosteric site on the channel.

Allosteric induction may explain subconductance state occurrence in acetylcholine receptor channels [26]. Jahr and Stevens [27] and Cull-Candy and Usowicz [28] have demonstrated subconductance states activated by the binding of amino acids to channels. Similarly, some toxin-enhanced substates (substates which occur normally, but infrequently) may be caused by conformational changes in pore size [3,23]. Prod'hom et al. [29] proposed that the binding of a proton to the L-type calcium channel could cause a conformational change in the channel which would cause a subconductance state, thus accounting for the pH sensitivity of the channel. The time scale ($< 10^{-4}$ s) in which this event naturally occurs seems to exclude it as a cause for subconductance states in the maxi-K channel which are able to last up to several seconds (see Fig. 3). Long-lived subconductance state occurrences have been seen in maxi-K channels from other preparations as well [6] and would indicate a more stable situation. Calcium is the major natural agonist which will bind to maxi-K channels. There may be an effect of calcium on subconductance state occurrence, but we have not clearly established this. Also, we have not examined the effect of magnesium or pH on subconductance state occurrence.

Random changes in pore size are compatible with the idea that proteins are capable of motions that cause tilting or twisting of channel subunits over a time scale of $10^{-12}$–$10^{0}$ s [30–33]. One can imagine a protein pore moving between relatively stable conformational states which give rise to discrete subconductance levels like the $f$ stops on a camera diaphragm. Such a model has been proposed for sodium channel subconductance states [34]. This model is congruous with our data. Further support for this model is the occasional occurrence of relatively smooth transitions from one subconductance state to another (see Fig. 6).

A variation of this theme would be that the subconductance states are caused by the binding of a permeant or impermeant ion within the channel [35,36]. We have no evidence that this is occurring in the maxi-K channel. However, it seems unlikely when one considers the number of subconductance states and the length of time that the channel may spend in a subconductance state.

(D) If the channel pore size does not change, apparent subconductance levels could be created by changes in the gating frequency that are beyond the bandwidth of normal kinetic measurements. This model is also plausible when one considers the time scale of motions in a large protein. There are technical limitations to our ability to test this model. Recordings like those in Fig. 1 17% (left) and 41% (left) could argue for this model, while recordings like Fig. 1 41%, 52%, and 72% (right) would argue against it as would the analog changes depicted in Fig. 6. We used the highest bandwidth available with our recording equipment (see Materials and Methods) and still saw these events. Also, when the channel entered a high frequency buzz mode, openings were always to full conductance. Since these openings are followed by our amplifier, subconductance states would have to involve much higher frequencies.

In conclusion, six subconductance levels have been identified in the maxi-K channel from airway smooth muscle. Subconductance states usually occurred more than 0.01% and less than 5% of the time. This is a significant fraction of channel open time (often several hundreds of milliseconds) and probably reflects important features of channel structure and/or gating. Our data can be best explained by a model in which the pore of the channel changes its size through conformational changes in the channel protein.

**Acknowledgements**

This work was supported by grants from the Alberta Heritage Foundation for Medical Research, the Canadian Medical Research Council and the Alberta Lung Foundation. We would like to thank Paul Labrecque for preparing our cells.

**References**

1 Barrett, J.N., Magleby, K.L. and Pallotta, B.S. (1982) J. Physiol. 331, 211–230.
2 Latorre, R. (1986) Ion Channel Reconstitution. (Miller, C., ed.), pp. 431–467. Plenum Press, New York.
3 Lucchesi, K. and Moczydlowski, E. (1990) Neuron 2, 141–148.
4 Magleby, K.L. and Pallotta, B.S. (1983) J. Physiol. 344, 585–604.
5 Methfessel, C. and Boheim, G. (1982) Biophys. Struct. Mech. 9, 35–60.
6 Richards, N.W., Lowy, R.J., Ernst, S.A. and Dawson, D.C. (1989) J. Gen. Physiol. 93, 1171–1194.

7 Singer, J.J. and Walsh, J.V. Jr. (1987) Pflügers Arch. 408, 98–111.
8 Weik, R., Lönnendonker, U. and Neumcke, B. (1989) Biochim. Biophys. Acta 983, 127–134.
9 Bosma, M.M. (1989) J. Physiol. 410, 67–90.
10 Geletyuk, V.I. and Kazachenko, V.N. (1985) J. Membr. Biol. 86, 9–15.
11 Krouse, M.E., Schneider, G.T. and Gage, P.W. (1986) Nature 319, 58–60.
12 Miller, C. (1982) Phil. Trans. R. Soc. Lond. B 299, 401–411.
13 Magleby, K.L. and Palletta, B.S. (1983) J. Physiol. 344, 605–623.
14 McManus, O.B. and Magleby, K.L. (1988) J. Physiol. 402, 79–120.
15 McCann, J.D. and Welsh, M.J. (1986) J. Physiol. 372, 113–127.
16 Marthan, R., Savineau, J.P. and Mironneau, J. (1987) Respir. Physiol. 67, 127–135.
17 Absher, M., Woodcock-Mitchell, J., Mitchell, J., Baldor, L., Low, R. and Warshaw, D. (1989) In Vitro Cell. Devel. Biol. 25, 183–192.
18 Hamill, O.P., Marty, A., Neher, E., Sakmann, B. and Sigworth, F.J. (1981) Pflügers Arch. 391, 85–100.
19 Stockbridge, N. (1987) Comput. Biol. Med. 17, 299–304.
20 Hille, B. (1984) Ionic Channels of Excitable Membranes. Sinauer Assoc., Sunderland, MA. 426 pp.
21 Benham, C.D., Bolton, T.B., Lang, R.J. and Takewaki, T. (1986) J. Physiol. 371, 45–67.
22 Fox, J.A. (1987) J. Membr. Biol. 97, 1–8.
23 Schreibmayer, W., Tritthart, H.A. and Schindler, H. (1989) Biochim. Biophys. Acta 986, 172–186.
24 Kazachenko, V.N. and Geletyuk, V.I. (1984) Biochim. Biophys. Acta 773, 132–142.
25 Matsuda, H., Matsuura, H. and Noma, A. (1989) J. Physiol. 413, 139–157.
26 Morris, C.E. and Montpetit, M. (1985) Can. J. Physiol. Pharmacol. 64, 347–355.
27 Jahr, C.E. and Stevens, C.F. (1987) Nature 325, 522–525.
28 Cull-Candy, S.G. and Usowicz, M.M. (1989) J. Physiol. 415, 555–582.
29 Prod'hom, B., Pietrobon, D. and Hess, P. (1987) Nature 329, 243–246.
30 Frauenfelder, H., Parak, F. and Young, R.D. (1988) Annu. Rev. Biophys. Biophys. Chem. 17, 451–479.
31 Lauger, P. (1985) Biophys. J. 47, 581–589.
32 Mizuji, E., Acerenza, L. and Lin, J. (1987) J. Theor. Biol. 129, 163–175.
33 Unwin, N. (1989) Neuron 3, 655–676.
34 Patlak, J.B. (1988) J. Gen. Physiol. 92, 423–430.
35 Pietrobon, D., Prod'hom, B. and Hess, P. (1988) Nature 333, 373–376.
36 Takeda, K. and Trautmann, A. (1984) J. Physiol. 349, 353–374.